4-1-2024

Enhanced carbohydrate-based plastic performance by incorporating cerium-based metal-organic framework for food packaging application

Shima Jafarzadeh

Mitra Golgoli
Edith Cowan University

Maryam Azizi-Lalabadi

Javad Farahbakhsh
Edith Cowan University

Mehrdad Forough

See next page for additional authors

10.1016/j.ijbiomac.2024.130899
Jafarzadeh, S., Golgoli, M., Azizi-Lalabadi, M., Farahbakhsh, J., Forough, M., Rabiee, N., & Zargar, M. (2024). Enhanced carbohydrate-based plastic performance by incorporating cerium-based metal-organic framework for food packaging application. International Journal of Biological Macromolecules, 265(Part 1), article 130899. https://doi.org/10.1016/j.ijbiomac.2024.130899

International Journal of Biological Macromolecules 265 (2024) 130899

Contents lists available at ScienceDirect

International Journal of Biological Macromolecules

journal homepage: www.elsevier.com/locate/ijbiomac

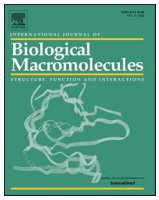

Enhanced carbohydrate-based plastic performance by incorporating cerium-based metal-organic framework for food packaging application

Shima Jafarzadeh [a], Mitra Golgoli [b], Maryam Azizi-Lalabadi [c], Javad Farahbakhsh [b], Mehrdad Forough [d], Navid Rabiee [e], Masoumeh Zargar [b,*]

[a] Centre for Sustainable Bioproducts, Deakin University, Waurn Ponds, VIC 3217, Australia
[b] School of Engineering, Edith Cowan University, 270 Joondalup Drive, Joondalup, WA 6027, Australia
[c] Research Center for Environmental Determinants of Health (RCEDH), Kermanshah University of Medical Sciences, Kermanshah, Iran
[d] Department of Chemistry, Middle East Technical University, 06800 Çankaya, Ankara, Turkey
[e] Centre for Molecular Medicine and Innovative Therapeutics, Murdoch University, Perth, WA 6150, Australia

ARTICLE INFO

Keywords:
Active packaging
Metal-organic framework
Nanoparticles
Biodegradable materials

ABSTRACT

The development of biodegradable active packaging films with hydrophobic characteristics is vital for extending the shelf life of food and reducing the reliance on petroleum-based plastics. In this study, novel hydrophobic cerium-based metal-organic framework (Ce-MOF) nanoparticles were successfully synthesized. The Ce-MOF nanoparticles were then incorporated into the cassava starch matrix at varying concentrations (0.5 %, 1.5 %, 3 %, and 4 % *w*/w of total solid) to fabricate cassava-based active packaging films via the solution casting technique. The influence of Ce-MOF on the morphology, thermal attributes, and physicochemical properties of the cassava film was subsequently determined through further analyses. Biomedical analysis including antioxidant activity and the cellular morphology evaluation in the presence of the films was also conducted. The results demonstrated that the consistent dispersion of Ce-MOF nanofillers within the cassava matrix led to a significant enhancement in the film's crystallinity, thermal stability, antioxidant activity, biocompatibility, and hydrophobicity. The introduction of Ce-MOF also contributed to the film's reduced water solubility. Considering these outcomes, the developed cassava/Ce-MOF films undoubtedly have significant potential for active food packaging applications.

1. Introduction

The packaging industry is the largest plastic user with over 90 % of flexible packaging made from plastic [1]. Plastics have seen exponential growth in the food packaging sector due to their cost-effectiveness and excellent resistance to mechanical and environmental factors [2]. Despite these advantages, plastic food packaging contributes significantly to global solid waste, with <12 % being recycled and approximately 95 % discarded after single use [3]. Petroleum-based plastic materials take centuries to break down, which poses a threat to the environment [5].

Plastic production and incineration are projected to substantially increase greenhouse gas emissions, soaring from 850 million tonnes in 2021 to 2.8 billion tonnes in 2050 [6,7]. Due to the negative impact of plastics on the environment, plastic usage should be reduced. One effective approach is shifting towards environmentally friendly food packaging materials. Numerous research studies have been performed in developing eco-friendly packaging based on biodegradable materials such as proteins and polysaccharides [9]. This sustainable shift in food packaging materials offers a promising solution to environmental challenges posed by plastics.

A wide range of biodegradable packages has been developed by utilizing natural materials such as polysaccharides (starch, chitosan, cellulose), proteins (wheat gluten, whey proteins, soy proteins, and fish proteins), or a combination of these materials [10, 11, 12]. Among these natural sources, starch has attracted significant interest in the packaging industry. It has excellent filming properties apart from its low cost and the absence of odor, taste as well as color. Cassava (*Manihot esculenta crantz*) is one of the most economical sources for producing cassava starch. Cassava starch as a biodegradable source [13], exhibits superior film-forming and casting properties due to its high amylose content (17 % *w*/w). Although cassava starch possesses excellent properties

* Corresponding author.
E-mail address: m.zargar@ecu.edu.au (M. Zargar).

https://doi.org/10.1016/j.ijbiomac.2024.130899
Received 16 December 2023; Received in revised form 12 March 2024; Accepted 12 March 2024
Available online 13 March 2024

Table 1
Summary of the recent studies incorporating different MOF nanomaterials into food packaging.

Nanomaterials	Base film	Properties	Ref.
Fe^{III}-HMOF-5[a]	Gelatin/chitosan	Fe^{III}-HMOF[c]-5 effectively controlled the hydrophobicity of capsaicin and successfully resolved the phase separation issue. It significantly enhanced the barrier properties.	[19]
Cu-MOF	Cellulose acetate	The nanocomposite films exhibited excellent compatibility with cellulose acetate while forming uniform and compact structures. These films demonstrated improved surface hydrophobicity, water vapor barrier ability and other functional properties compared to unmodified cellulose acetate film. Additionally, they displayed outstanding UV shielding properties across the entire UV range.	[20]
Ag-MOFs	Chitosan	The incorporation of Ag-MOFs in chitosan demonstrated their immense potential in the cost-effective and eco-friendly preservation of fresh fruits.	[21]
MOF-801[b]	cyclic olefin copolymer	The films exhibited improved water vapor transmission rates and hydrophobicity.	[22]
Co-MOF[c]	sodium alginate	The uniform distribution of Co-MOF nanofillers in the matrix resulted in significant enhancements in the film's tensile strength, toughness, thermal stability, UV-shielding and water vapor barrier capabilities.	[23]
Zn-MOF	chitosan–polyethylene glycol	The results demonstrated the improvement in the film's tensile strength, antibacterial activity and thermal stability.	[24]

[a] Fe^{III} doped hollow MOFs.
[b] $Zr_6O_4(OH)_4(fumarate)_6$.
[c] Cobalt-based metal-organic framework.

comparable to petroleum-based plastics, it has limitations such as high permeability [14,15].

Porous materials have recently drawn considerable attention due to their large surfaces, peculiar structures, gas barrier properties, thermal stability, and flexibility in functionalization. A metal-organic framework (MOF) is a crystalline porous material structure formed by coordinative bonds between metal clusters and organic ligands. Additionally, MOFs are considered a cutting-edge material for the adsorption of toxic compounds because of their high porosity, surface area and modulation stability [16]. Previous studies have demonstrated that highly efficient films can be produced with the incorporation of MOF nanomaterials (Table 1).

Rare earth elements such as cerium-based metal-organic frameworks (Ce-MOFs) have gained considerable popularity in the last few years due to their exceptional physicochemical properties and environmental friendly [17]. They could be used in various applications due to improved material characteristics. The binding affinity, structure tunability, stability, magnetic properties, and photocatalytic activity of cerium (Ce)-based materials are some of the most promising among the rare earth elements [18]. Despite the environmental sustainability and unique properties of Ce-MOF, their effect on biodegradable food packaging has not been studied.

The present study aimed to develop active biodegradable packaging reinforced with porous nanomaterials and investigated the role of porous materials in enhancing the performance of biopolymer films. For the first time, Ce-MOF were incorporated into natural packaging material for food packaging applications. The morphology as well as the thermal and physicochemical properties of the biomaterials were determined. Besides offering the same advantages of plastic packaging (low cost, high resistance to heat and moisture), this innovative food packaging could reduce the use of petroleum-based plastic.

2. Experimental section

2.1. Materials

All chemicals and materials used in this study were of analytical grade and were utilized without further purification. 5-aminoisophthalic acid (≥98 %; 5AIPA), ethanol (99.9 %), *N*,*N*-Dimethylformamide (DMF), acetone, and methanol (≥99.8 %) were procured from Merck (Darmstadt, Germany). Cerium (III) chloride heptahydrate ($CeCl_3.7H_2O$) and sorbitol were obtained from Sigma-Aldrich. Cassava flour was sourced from a local market.

2.2. Cerium-based metal-organic framework synthesis

The solvothermal synthesis of Ce-based MOFs was conducted following a modified procedure described in the literature with some modifications [25]. Initially, 3.60 mmol of 5AIPA was dissolved in 13.2 mL DMF to obtain a transparent solution. Subsequently, 1.8 mmol of $CeCl_3.7H_2O$ was added to the solution. The mixture was then stirred and sonicated for 20 min until a homogeneous solution was achieved. The resulting solution was then transferred into a stainless steel autoclave and heated at 160 °C for 72 h. After cooling overnight at room temperature, the resulting crystalline beige powder was separated by centrifugation (12,000 rpm), and the mother liquor was decanted. To activate the MOF crystals and remove the reaction solvent (DMF) from the pores, the Ce-MOF was thoroughly washed several times with DMF and methanol in the final step. Finally, the material was dried at 120 °C under vacuum.

2.3. Bio-nanocomposite film fabrication

Cassava flour (3.5 g) and distilled water (80 mL) were mixed by magnetic stirring at room temperature. Various concentrations of the synthesized Ce-MOF powder (0.5 %, 1 %, 1.5 %, 3 %, and 4 % *w*/w of total solid) and 40 % w/w of sorbitol were dispersed in 20 mL of distilled water and ultrasonicated (Marconi model, Unique USC 45 kHz, Piracicaba, Brazil). The dispersions of cassava flour, Ce-MOF and plasticizer were then mixed and stirred at 90 °C for 30 min. The homogeneous mixtures were poured onto plates and allowed to evaporate for 24 h. Similar steps were performed during the preparation of a control film apart from the addition of nanoparticles. The dried films were peeled and stored at 23 ± 2 °C and 55 % relative humidity until further use. Fig. 1 illustrates the film fabrication procedure.

2.4. Cerium-based metal-organic framework characterization

X-ray diffraction (XRD) analysis was conducted using a PANalytical Empyrean diffractometer, operating at 40 kV voltage and 40 mA current, with Co-kα radiation (λ = 0.1789 nm). Fourier transform infrared spectroscopy (FTIR) was performed in the range of 450–4000 cm^{-1} using a PerkinElmer spectrometer. Additionally, the zeta potential of MOFs was measured via a ZEN3600 Zetasizer (Malvern Instruments Co., Ltd., U.K.).

2.5. Bio-nanocomposite film characterization

The selected films were subjected to Attenuated Total Reflection–Fourier transform infrared spectroscopy (ATR-FTIR Spectrometer,

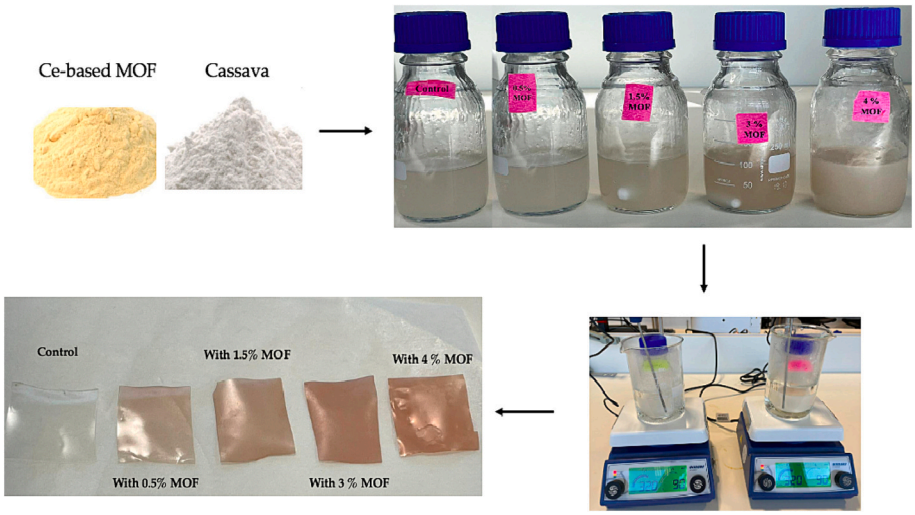

Fig. 1. Fabrication procedure of the Cerium-based metal-organic framework integrated Cassava active packaging films.

Perkin Elmer). The thin films were applied directly to a ZnSe ATR cell, which was then clamped into the FTIR spectrometer mount. Spectral noise was reduced by averaging 64 consecutive scans at 4 cm^{-1} resolution for each spectrum. XRD patterns of the films were obtained at a rate of 0.01°/s using a PANalytical EMPYREAN diffractometer. Film surface morphologies were determined by scanning electron microscopy (SEM, FEI Verios 460). The samples were dried overnight and affixed to aluminium stubs using double-sided copper tape. Subsequently, a 10 nm platinum coating was applied using Polaron SC7640 (Quorum Technologies, UK) prior to imaging. SEM imaging of the samples was carried out in a voltage range of 5–10 kV, maintaining a working distance of 5.5 mm. Using a thermogravimetric analyzer (TGA-1, Perkin Elmer, Massachusetts, USA), samples (15 mg) were heated from 40 to 800 °C under nitrogen with a heating rate of 10 °C/min. The hydrophilicity of films was measured under ambient conditions using an Attention Theta Optical Tensiometer. The surface of the film was sprayed with 5 mL of water using a syringe. Following the release of water onto the film surface, images were taken and documented immediately. The angle between the drop boundary and the tangent was measured. In order to calculate the mean value, five measurements were performed on the films. Roughness and 3D morphology of the surfaces of films were analysed by atomic force microscopy (AFM, Nanosurf model C3000). To determine the thickness of each film, a precision digital micrometre (Mitutoyo, Kanagawa, Japan) was used. The mean value was calculated for each film. The solubility of nanocomposite films was tested according to the literature [26]. The dehydrated film pieces (2.5 × 2.5 cm^2) were measured to the nearest 0.0001 g in a desiccator containing phosphorus pentoxide (0 % RH) at ambient temperature (25 °C for 3 days). Initially, the samples were stirred (1 h, 40 rpm) in deionised water (80 mL, 18MX). Filtration (Whatman No. 1) was performed to separate the remaining pieces of the film. A constant weight was obtained by drying the remaining pieces at 60 °C for 24 h, followed by calculating the weight of the dried insoluble material. To determine the weight of water-soluble materials, all insoluble and non-soluble materials were deducted. All tests were performed in triplicates. Film solubility (FS%) was calculated using the following formula:

$$\text{Film Solubility}: FS\% = \frac{\text{Wi} - \text{Wf}}{\text{Wi}} \times 100 \quad (1)$$

where W_i is the initial dry film weight (g) and W_f is the final dry film weight (g).

In order to determine the moisture content, approximately 50 mg of the bio-nanocomposite films were kept at room temperature (58 % RH, 25 °C) for two days. The bio-nanocomposite films were then dried for 1 day at 105 °C to obtain an equilibrium weight. Moisture content was calculated using the following equation:

$$\text{Moisture content}: x = \frac{\text{Mi} - \text{Mf}}{\text{Mi}} \times 100 \quad (2)$$

where M_i and M_f represent the initial and final weights of the dried samples, respectively. Each film was tested in triplicates.

2.6. Antioxidant activity

The antioxidant properties of the prepared MOF-based films were determined by measuring their ability to neutralize DPPH free radicals. The specific methods were outlined by Jridi et al. [27] and Rabiee et al. [28]. Approximately 20 mg of small film pieces were cut and placed in 4 mL of methanol solution containing 2,2-diphenyl-1-picrylhydrazyl (DPPH) at a concentration of 0.1 mM. This mixture was then incubated at room temperature for different periods of time. The absorbance of the solution was measured at 517 nm using a microplate reader (Varioskan LUX). The percentage of DPPH scavenging activity for all the sample films and butylated hydroxytoluene (BHT) was determined by Eq. (3):

$$\text{DPPH scavenging activity}\ (\%) = \frac{\text{Control absorbance} - \text{Sample absorbance}}{\text{Control absorbance}} \times 100 \quad (3)$$

2.7. Cell behavior evaluation

The cellular behavior and morphology were monitored by 2D fluorescent microscopy to assess the potential interaction between the newly synthesized MOF-based films and their impact on cell death. 1 × 10^5 cells per well were seeded onto each sample while placing the substrates in Dulbecco's Modified Eagle's Medium (DMEM, Gibco) supplemented with 100 IU/mL of streptomycin, 100 IU/mL of penicillin (both from Invitrogen) and 10 % fetal bovine serum (FBS, Gibco). The cell suspension was then incubated at 5 % CO_2 and 37 °C. At each time point, 100 μL of MTT solution (5 mg/mL in PBS) was added to each well. After a 4-h incubation, the culture was removed and the formazone precipitate was dissolved in dimethyl sulfoxide. The absorbance at 570 nm ($n = 3$) was measured using a microplate Elisa reader. The 2D fluorescence microscopy was used to investigate cell morphology in the presence of these newly synthesized MOF-based films. Specifically, the SW480 (CCL-228) cells were selected as the control group to observe cellular morphology before and after interaction with the films. SW480 cells

were seeded in a 96-well plate at a density of 2×10^5 cells per well and incubated for over 24 h. The medium with MOF-based film (highest concentration) was replaced to maintain the amount of MOF-based film. After a 4-h incubation, the cell suspensions were treated with 4′,6-diamidino-2-phenylindole (DAPI) for 15 min following several washes and fixation with 4 % paraformaldehyde.

2.8. Statistical analysis

Bio-nanocomposite film properties were compared using analysis of variance and Duncan post-hoc tests (at a 5 % significance level). The statistical analyses were carried out using SPSS version 22.0.

3. Results and discussion

3.1. MOF characterization

As shown in Fig. 2A, the crystallinity of the synthesized Ce-MOF was thoroughly examined using powder X-ray diffraction. The presence of sharp and distinct diffraction peaks indicates a highly ordered and structured phase [29]. The XRD pattern of Ce-MOF demonstrated strong diffraction peaks at 2θ values of 11.68°, 19.94°, 20.47° and 23.48°. FTIR spectra of synthesized Ce-MOF are presented in Fig. 2B. In the pure Ce-MOF spectrum, the peaks appearing at 1466 cm^{-1} and 1378 cm^{-1} correspond to the stretching vibrations of the COO^- groups. As shown in Fig. 2B, low-intensity peaks were observed at 729 cm^{-1} and 549 cm^{-1} wavenumbers, which are associated with Ce—O stretching vibrations [29]. The peak at 1552 cm^{-1} is related to C═O vibration, which confirms the presence of DMF in the Ce-MOF nanocrystal and indicates that the framework is reinforced due to the existence of adsorbed solvent molecules. All these observed peaks collectively demonstrate that the Ce-metal is coordinated with the imidazole ligand, affirming the successful synthesis of Ce-MOF. The result indicated a zeta potential of 4.21 ± 0.63 mV.

3.2. Bio-nanocomposite film characterization

3.2.1. Thickness

Based on the findings of this study, the different concentrations of nanofiller did not significantly affect biopolymer film thickness. The nanocomposite films (0.17 ± 0.05 mm) were significantly thicker ($p < 0.05$) than the control films (0.14 ± 0.05 mm). The thickness of films containing Ce-MOF was higher at all levels ($p < 0.05$) than the thickness of films without nanofillers. It was likely due to the nanofillers placed between the matrix networks as well as the high solid content of the resulting films [30].

3.2.2. X-ray powder diffraction (XRD) analysis

The impact of blending and integration on the crystalline structures of the substrates was illustrated by the XRD spectrum [31,32]. Fig. 3 shows the XRD profiles of pure film and films containing 0.5, 1.5, 3, and 4 % of Ce-MOF nanocrystals. Based on the Scherrer mathematical statement ($\tau = \kappa \lambda/\beta \cos\theta$), the mean crystallite size of the nanocrystal was estimated to be 50 nm. In this calculation, τ is the mean crystalline size, κ is a constant relevant to the shape agent (about 0.9), λ is the wavelength of X-ray radiation, β is the full width at half the maximum intensity and θ is the Bragg diffraction angle [33]. The mean crystallite size was in accordance with the mean granule size estimated from SEM. As shown in Fig. 3, the intensity of the peaks increased at certain 2θ values with the increase in crystalline structure of the compounds. Whereas a semi-crystalline structure increased the width of the peak. The intensity of the cassava flour peaks was not high. The diffraction peak spectrum was found to be non-uniform without having a sharp specified peak, which indicated the amorphous structure of cassava flour. Upon adding Ce-MOF nanocrystals to cassava flour, distinct peaks around $2\theta = 8.5–11.5°$ were observed. Furthermore, diffraction peaks at 2θ values of 20.47° and 23.48° indicated the presence of Ce-MOF (Fig. 3). The intensity of these peaks increased with the increase in Ce-MOF concentrations (3 % and 4 %). Based on previous research [27], the crystallinity of cassava granules was observed at $2\theta = 20°$, which represented the interaction between the amylose and the amylopectin after the gelatinization procedure.

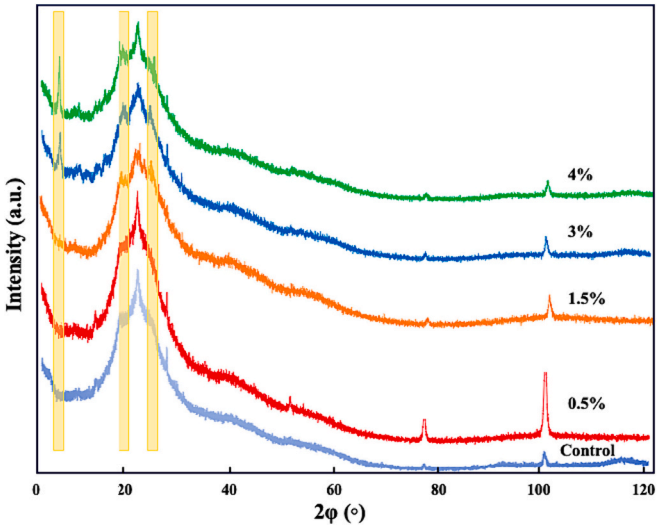

Fig. 3. The standard X-ray Powder Diffraction spectra of 0.5, 1.5, 3, and 4 w/w % metal-organic framework nanocrystal integrated cerium-based films.

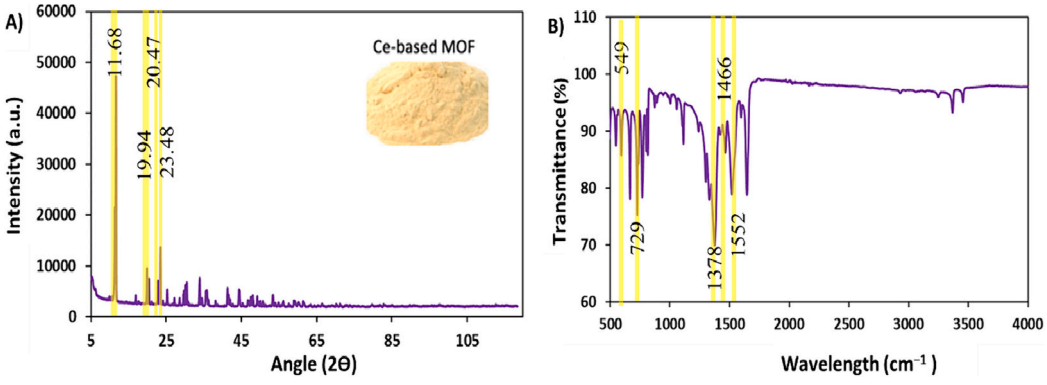

Fig. 2. (A) XRD patterns of Ce-MOF and (B) FTIR spectrum of Ce-MOF.

3.2.3. Scanning electron microscope (SEM) analysis

The structure, morphology, and homogeneity of a matrix can influence the properties of film, particularly barrier properties [34]. Surface and cross-sectional morphologies of the pure film and film loaded with Ce-MOF nanocrystals at different concentrations are displayed in Fig. 4. Uniform surface morphology is shown for cassava flour as a control sample, and gradually rough and harsh structure is seen for the 0.5, 1.5, 3 and 4 % Ce-MOF nanocrystals, especially in the surface SEM images which is in accordance with that of Shahabi-Ghahfarrokhi et al. [48]. However, no aggregation or accumulation of Ce-MOF nanocrystals was observed in 3 and 4 % concentrations, which indicated the uniform distribution of Ce-MOF structure. In previous research [35–37] polymer films had pores and fractures resulting from low concentrations of substances, especially in the cross-sectional area. However, at higher concentrations, the greater interaction between substances and/or polymer networks reduced the fractures.

As can be seen in our study, at the 0.5 % Ce-MOF loading, fractures were observed in the cross-sectional SEM micrographs, which appear mitigated in the 4 % specimen micrographs. Monteiro et al. (2018) evaluated the effect of bentonite clay in cassava flour. They reported that a high concentration of bentonite could significantly decline homogeneity of the cassava flour film surface. Moreover, no accumulation was observed in polymeric matrix [33].

3.2.4. Contact angle

Packaging with high hydrophobic characteristics can provide significant benefits to food products that are sensitive to moisture or water.

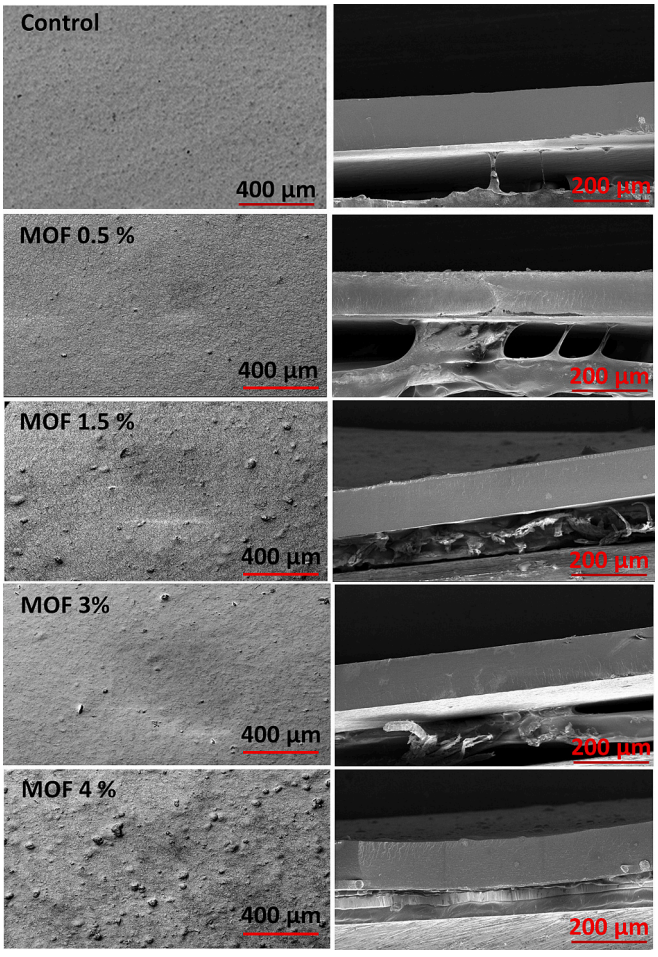

Fig. 4. SEM microstructure of the surface (left side) and cross-section (right side) cassava film incorporated with 0.5, 1.5, 3 and 4 % cerium-based metal-organic framework nanocrystals.

Hydrophobic packaging materials act as effective barriers to moisture absorption. Such packaging is particularly advantageous for food products susceptible to spoilage, rancidity, or degradation caused by moisture [15,38].

The contact angles evaluation for water droplets on the surface area of cassava biopolymer film are shown in Fig. 5A. As the control treatment, the contact angle for cassava film was 62.205°, which showed surface hydrophilicity being in good agreement with previous studies [39–41]. The contact angle in cassava film with 0.5, 1.5, 3, and 4 % Ce-based MOF nanocrystal were determined to be 81.2, 87.65, 89.95 and 91.8°, respectively. The incorporation of Ce-based MOF increased the contact angle of water droplets in the cassava polymeric matrix and raised the hydrophobicity characteristics. Jantanasakulwonget al. also reported similar outcomes as per our results [39]. The increase in Ce-based MOF nanocrystals affected the hydrophobicity by the interaction between cassava and Ce-based MOF nanocrystals as well as increased the contact angle. In fact, the competition between water droplets and cassava chains in the nanocrystal structure enhanced the hydrophobicity.

3.2.5. Thermal gravimetric analysis (TGA)

Various industrial applications such as food packaging require materials with high thermal stability. Due to their exceptional thermal stability, porous nanomaterials (PNMs) have attracted considerable attention in recent years. A number of factors such as the nature and position of functional groups, the metal hardness and the coordination of solvent molecules could influence the thermal stability [42]. The impact of different concentrations of Ce- MOF nanocrystals (with 0.5, 1.5, 3, and 4 %) on the thermal stability and weight retention of cassava film is presented in Fig. 5B. The first thermal degradation of pure cassava starch occurred between 30 and 120 °C, as a result of water molecules being physically absorbed. In the second weight loss process, glycerol and other low molecular weight compounds decompose between 150 and 300 °C. Final weight loss occurred due to decomposition and fracture of functional groups in cassava starch at temperatures between 340 and 480 °C. Ce-based MOF nanocrystal addition changed the thermal degradation behavior of cassava starch composites [35,43]. Well-dispersed Ce-based MOF acts as a physical barrier and slowing thermal decomposition. Moreover, MOF can initiate polymer crystallization during processing, increasing crystallinity and strengthening matrices against thermally induced chain breakdown. As shown in Fig. 5B the final mass was higher for films contained Ce-based MOF nanocrystal as they included more inorganic material that was difficult to volatilize at the temperatures used. In the initial stage, the Ce-based MOF-added composite films exhibited slower degradation, while, in the second stage, the thermal decomposition rate increased with higher Ce-based MOF content, possibly due to the gradual removal of hydroxyl and carboxyl groups at temperatures below 350 °C. In the third stage, the thermal decomposition of the starch composites decreased due to the formation of intermolecular hydrogen bonding between the functional groups in Ce-based MOF and the matrix. The high thermal stability of cassava-Ce-based MOF nanocrystal film is related to the strong connection between nanocrystal particles and polymeric networks. Similar results were obtained by Khan et al. (2021). They conducted TGA to assess the impact of -MOFs on the thermal stability of films from 25 to 600 °C. Increasing the loading rate of ZIF-67 in polyvinyl alcohol and starch composites resulted in a decrease in weight loss. However, the ZIF-67 decomposed when the temperature reached 450 °C. Therefore, MOFs could be used to improve composite materials' thermal stability [44].

3.2.6. Fourier-transform infrared spectroscopy

Fig. 6 shows the FTIR spectra of cassava flour incorporated with 0.5, 1.5, 3, and 4 % concentrations of Ce-based MOF nanocrystal. A peak for cassava flour appeared at 3200–3400 cm^{-1}, which is related to the stretching of hydroxyl group (-OH) with hydrogen connection. The peak

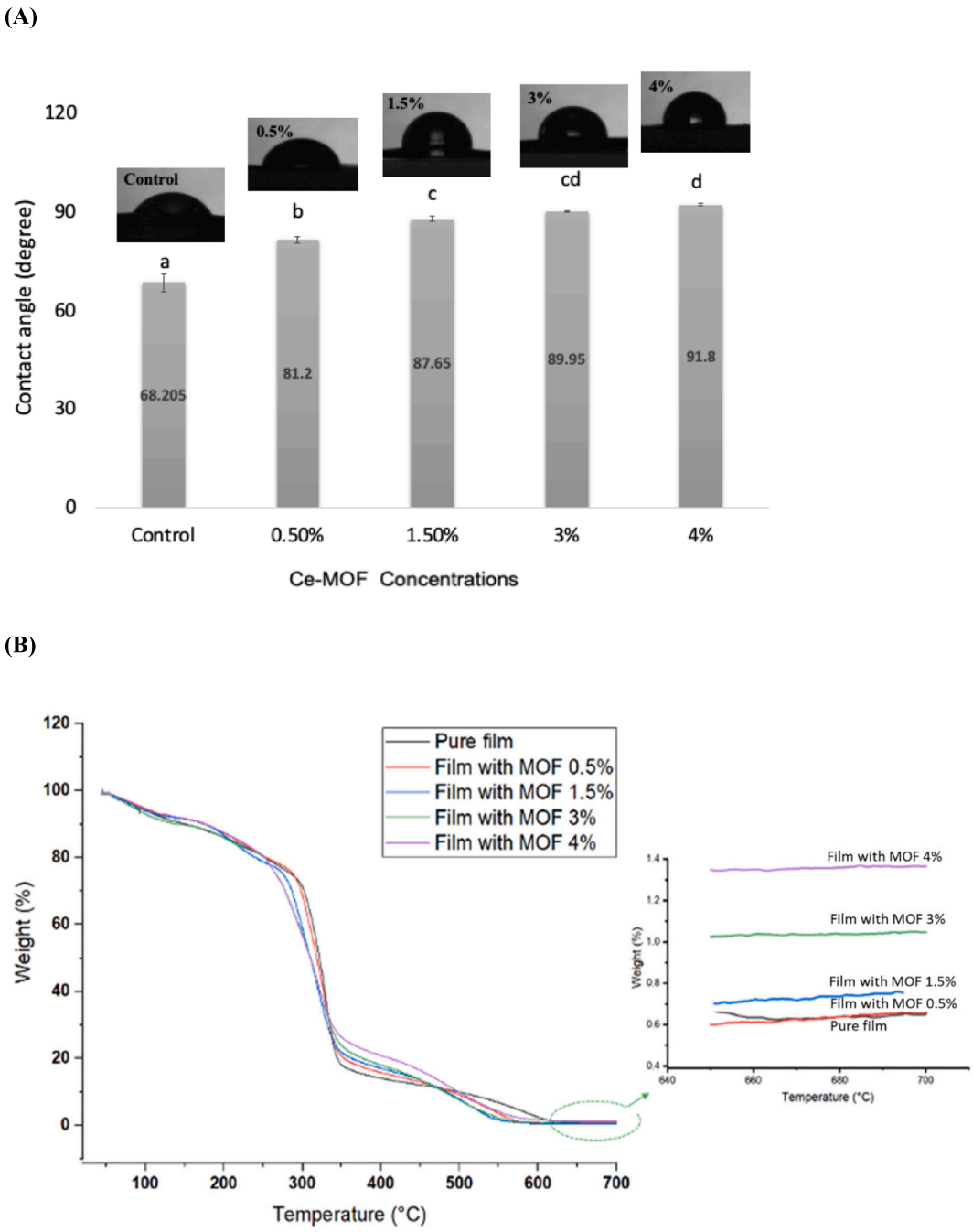

Fig. 5. (A) The contact angle of water droplet on cassava film with different concentration of cerium-based metal-organic framework nanocrystals and (B) thermal gravimetric analysis of the different concentration of cerium-based metal-organic framework nanocrystals.

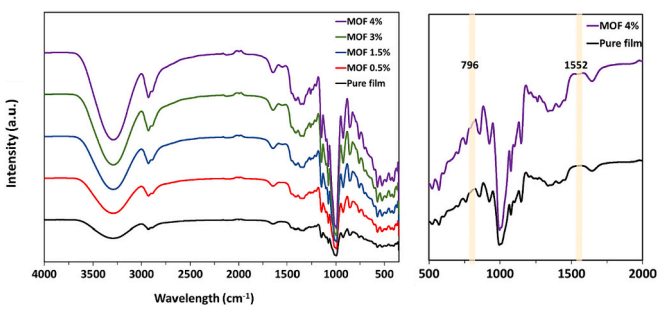

Fig. 6. FT-IR spectra of different concentrations of cerium-based metal-organic framework nanocrystals.

at wavenumber around 3000 cm^{-1} is related to the C—H stretch [41,43]. The peak at wavenumber between 800 and 1100 cm^{-1}, is associated with C—O, C—C, and C—O—H vibrations. The FTIR spectra exhibit minimal changes in absorption band shapes and intensities following Ce-MOF addition, indicating uniform incorporation without substantial structural alterations. Retention of the characteristic cassava vibrations along with the formation of unique stretches related to Ce-MOF signifies effective interfacial bio-interactions arising from novel crosslink formation between the nanocrystals and biopolymer matrix [18,33]. At 796 cm^{-1} wavenumber, a low-intensity peak was observed, which was associated with Ce—O stretching vibrations (Fig. 6). The identification of a peak at 1552 cm^{-1}, associated with C═O vibration, verifies the use of DMF in Ce-MOF nanocrystal synthesis. This is further supported by the presence of strongly adsorbed solvent molecules. The

interaction of water molecules with Ce-based MOF nanocrystal resulted in the appearance of a peak at 3450 cm^{-1} (OH stretching) [18].

3.2.7. AFM analysis

AFM is an effective tool for studying the surface roughness of materials at the nano-meter scale. It can provide quantitative and qualitative information about biopolymers that cannot be obtained by any other experimental method [45]. The structural differences in films can be identified using AFM. Fig. 7 shows the surface morphologies and the surface roughness parameters (*Sa* and *Sq*) of the neat film and film with various Ce-MOF concentrations. The neat film exhibited a smooth surface whereas the film with a lower concentration of Ce-MOF (0.5 %) exhibited a relatively rough surface with Sa and Sq values of 58.68 and 70.65 nm, respectively. With the increase in Ce-MOF content, the film surface became rougher. The AFM image showed that cassava films with Ce-MOF 4 % were rougher, as reflected by higher Sa and Sq values (81.30 and 102.24 nm). The results of this study are consistent with those of Zhang et al. [21] for polyvinyl alcohol film with chitosan nanoparticles and Ag@MOF [17]. The authors stated that with the addition of Ag@MOF, the film's average roughness (Sq) increased. The peaks and valleys were observed in the 3D image. The sharp morphology of Ag@MOF and chitosan derivatives may confirm this.

3.2.8. Water solubility (WS) and moisture content (MC)

Water solubility is considered an essential indicator of water resistance. It is commonly believed that higher water solubility implies a lower water resistance of the film. As shown in Fig. 8, the incorporation of Ce-MOF into neat film reduced nanocomposite films' moisture content and water solubility compared to the neat films. It indicated that the addition of Ce-MOF improved the water resistance of the film. A slight reduction in the solubility of films from 8.47 to 5 was observed. Moreover, the moisture content reduced from 30.22 to 22.28. The change in water affinity is due to the presence of strong hydrogen bonds between the biopolymer matrix and the nanomaterials. This result is further supported by Zhang et al. [21]. They showed that the addition of Ag@MOF to chitosan and polyvinyl alcohol reduced the WS and MC [21]. Similarly, Feng et al. [23] reported that loading Co-MOF into sodium alginate-based film reduced the moisture absorption of neat films from 14.3 % to 10.2 %. The composite films have better water barrier abilities than neat films, which could be attributed to the tortuous path of moisture diffusion caused by the Co-MOF within the control matrix [23].

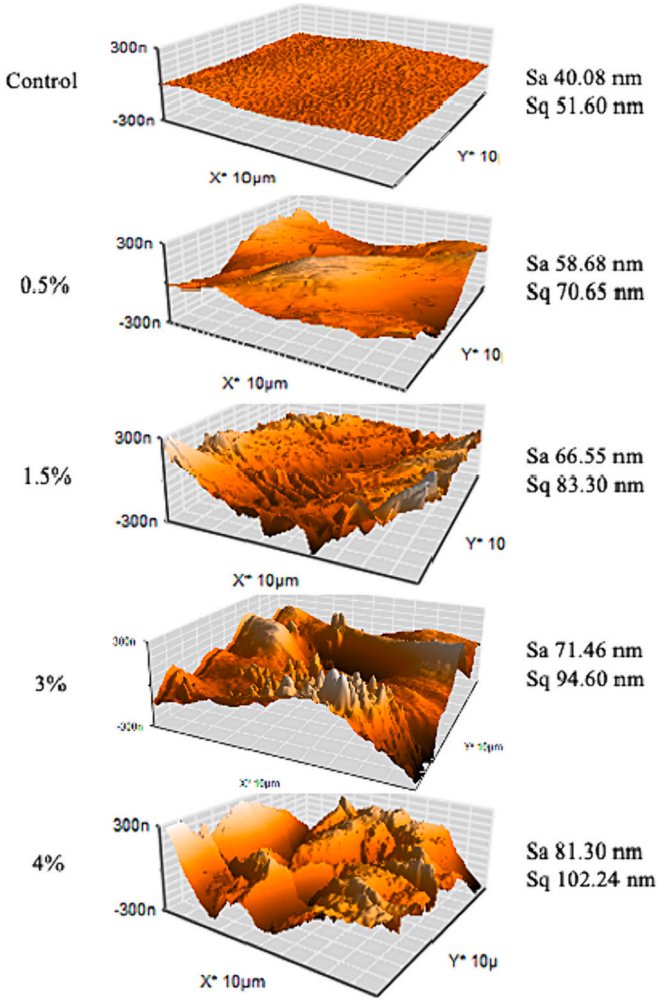

Fig. 7. AFM images of control film and bio-nanocomposite films integrated with different concentrations of cerium-based metal-organic framework.

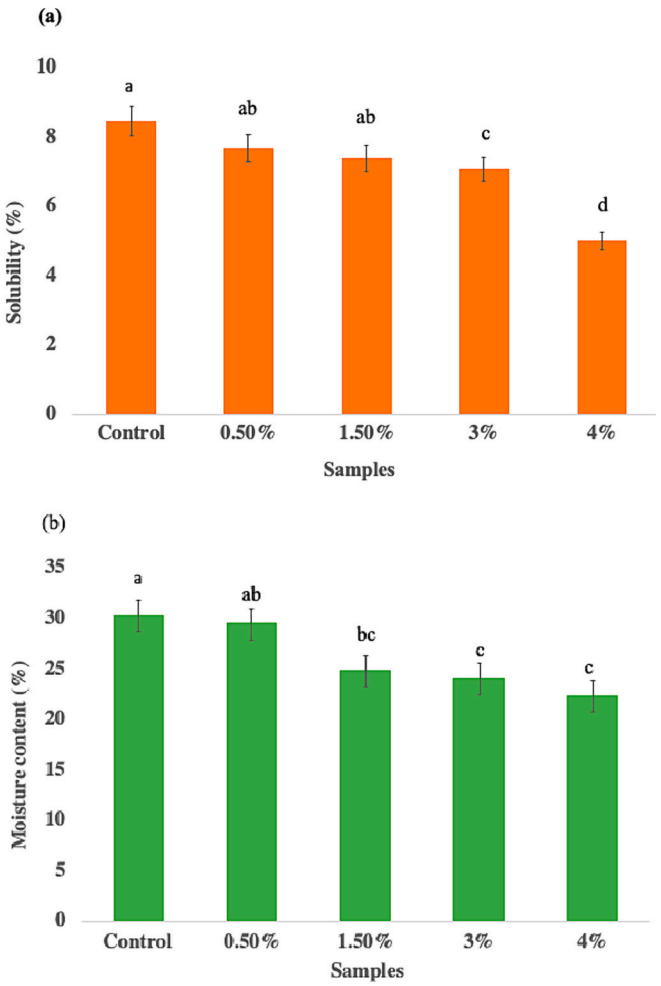

Fig. 8. (a) Water solubility and (b) moisture content of control cassava film and bio-nanocomposite cerium-based metal-organic framework integrated cassava films.

3.3. Antioxidant activity

The antioxidant potential of MOFs could be attributed to their unique structure having metal nodes connected by organic linkers, which result in high porosity and surface areas. This architecture allows the incorporation or encapsulation of antioxidant agents and facilitates their controlled release [46]. Certain MOFs have demonstrated intrinsic antioxidant properties due to the redox activity of the metal centers or the organic linkers. For instance, MOFs containing copper or manganese

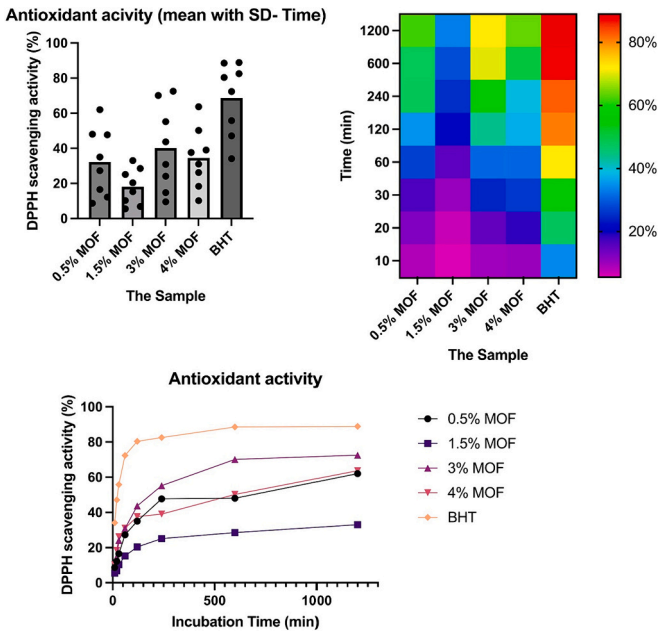

Fig. 9. Antioxidant activity (mean with SD-time) of the 0.5 % MOF, 1.5 % MOF, 3 % MOF, 4 % MOF, and compared to the BHT. All the graphs were designed by GraphPad Prism, based on the DPPH scavenging activity (%) and up to 1200 min.

metal centers have shown promise in catalytically dismutating superoxide radicals. Furthermore, MOFs can be engineered to release antioxidant molecules in response to specific stimuli. This can be achieved by post-synthetic modification or by designing stimulus-responsive MOFs. The controlled release of antioxidants ensures an enhanced therapeutic effect, reduced side effects, and better biocompatibility. For instance, MOFs have been designed to release antioxidants like glutathione or vitamin C under specific pH conditions or in the presence of certain enzymes while providing targeted therapeutic responses. In this study, four different concentrations of MOFs were evaluated and showed promising antioxidant activity compared to the control group (BHT) (Fig. 9). Cerium can exist in multiple oxidation states, with Ce(III) and Ce(IV) being the most stable. The ability of cerium to shuttle between these two oxidation states allows it to act as a redox-active center. In the presence of ROS, Ce(III) can be oxidized to Ce(IV) by capturing the free radicals and this oxidized form can later be reduced. This redox cycling property makes cerium a potent antioxidant. At varying concentrations of the Ce-MOF, the number of available redox-active cerium sites changes. A higher number of cerium sites are available to neutralize ROS at higher concentrations. However, the antioxidant efficiency might not increase proportionally beyond the saturation point. The 5-aminoisophthalic acid could engage in hydrogen bonding or other interactions with ROS due to its amine functionality, thereby enhancing the antioxidant property of the MOF. This linker may not only provide structural support but also synergistically enhance the redox activity of cerium. The presence of a higher number of linkers means a denser network of ROS interaction sites. In addition, a higher concentration of Ce-MOFs would intuitively mean more available active sites. There might be aggregation or stacking of MOF particles at too high concentrations, leading to decreased surface area exposure and reduced accessibility to ROS. Thus, an optimal concentration is necessary that can maximize antioxidant activity by balancing the number of active sites with the available surface area. Also, the kinetics of ROS neutralization can change at different concentrations. Higher concentrations initially provide faster ROS scavenging due to the increased number of active sites. However, beyond a certain concentration, the efficiency might plateau or even decrease due to aggregation or reduced accessibility [28].

3.4. Cellular behavior evaluation

The evaluation of potential therapeutic agents or materials often requires an understanding of their effects on cellular morphology [47]. The study on SW480 cells with the 4 % Ce-MOF film offers an insightful glimpse into the biocompatibility and potential safety of this particular material. One of the primary concerns in introducing any external agent to a biological system is its compatibility with living cells. The SW480 cells stained with DAPI showed no significant morphological changes upon treatment with the 4 % Ce-MOF film (Fig. 10). This suggests that

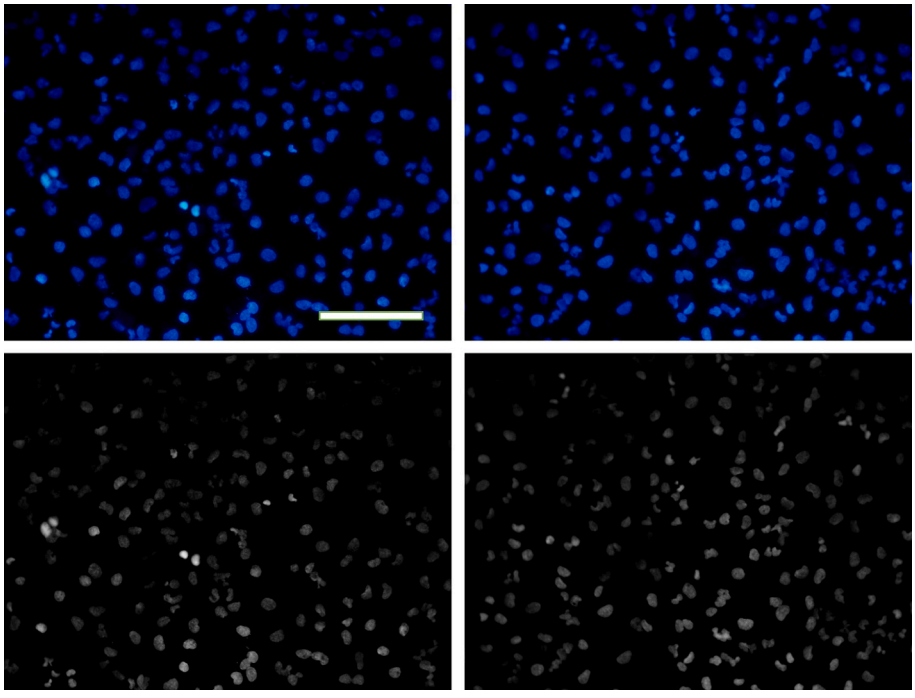

Fig. 10. Cellular morphology of the SW480 cell line stained with DAPI treated with the film containing 4 % Ce-MOFs. The scale bar is 50 μm.

the Ce-MOF film does not induce cytotoxic effects that could compromise cellular structure. Such biocompatibility is crucial, especially if this material is to be considered for biomedical applications or drug delivery systems. Also, cellular aggregations, which can arise due to external stimuli, often indicate stress responses or adverse reactions. Such aggregations might alter cell-to-cell communication, disrupt cellular functions, or even lead to cell death. The absence of such aggregations in SW480 cells post-treatment underscores the benign interaction of the Ce-MOF film with the cellular environment. In addition, the unchanged morphology of SW480 cells indicates that the 4 % Ce-MOF film remains chemically stable in the cellular environment, or at least, any release from the MOF does not adversely affect the cells.

4. Conclusion

The synthesis of novel Ce-MOF nanoparticles was performed in this research and an advanced cassava-based active food packaging system was developed. The integration of Ce-MOF nanofillers within the cassava matrix was found to be homogeneously dispersed, which led to significant improvements in various properties of the cassava film. There was a noticeable boost in thermal stability, hydrophobicity, biocompatibility, antioxidant activity, crystallinity, and solubility. Furthermore, our study elucidated that as the concentration of Ce-MOF in the matrix increased, there was a corresponding enhancement in the thermal stability and hydrophobicity of the film. This study demonstrates the promising potential of cassava/Ce-MOF composite films for various food packaging applications. While our investigation primarily focused on assessing the thermal stability, hydrophobicity, biocompatibility, and antioxidant activity of these films, several avenues for future research could further enhance their utility and effectiveness in food packaging. One potential direction for future study is to evaluate the antimicrobial activity of the developed films on food products and explore their suitability for use in food packaging applications. Additionally, future investigations might delve deeper into optimizing the Ce-MOF concentration for other desirable traits, exploring potential biodegradability advantages, and assessing their safety profile in food-contact scenarios.

CRediT authorship contribution statement

Shima Jafarzadeh: Writing – original draft, Validation, Methodology, Investigation. **Mitra Golgoli:** Writing – original draft, Methodology, Investigation. **Maryam Azizi-Lalabadi:** Writing – review & editing, Writing – original draft. **Javad Farahbakhsh:** Validation, Methodology. **Mehrdad Forough:** Writing – review & editing, Validation, Conceptualization. **Navid Rabiee:** Writing – review & editing, Validation. **Masoumeh Zargar:** Writing – review & editing, Validation, Supervision, Project administration, Conceptualization.

Declaration of competing interest

The authors declare that they have no known competing financial interests or personal relationships that could have appeared to influence the work reported in this paper.

Data availability

Data will be made available on request.

References

[1] S. Jafarzadeh, M. Hadidi, M. Forough, A.M. Nafchi, A. Mousavi Khaneghah, The control of fungi and mycotoxins by food active packaging: a review, Crit. Rev. Food Sci. Nutr. 63 (2023) 6393–6411.
[2] S. Jafarzadeh, Z. Yildiz, P. Yildiz, P. Strachowski, M. Forough, Y. Esmaeili, M. Naebe, M. Abdollahi, Advanced macromolecular technologies in biodegradable packaging using intelligent sensing to fight food waste; a review, Int. J. Biol. Macromol. 261 (2024) 1–23.
[3] F. Garavand, M. Rouhi, S. Jafarzadeh, D. Khodaei, I. Cacciotti, M. Zargar, S. H. Razavi, Tuning the physicochemical, structural, and antimicrobial attributes of whey-based Poly (L-Lactic Acid) (PLLA) films by chitosan nanoparticles, Front. Nutr. 9 (2022) 880520.
[5] D. Hermawan, T.K. Lai, S. Jafarzadeh, D.A. Gopakumar, M. Hasan, F.A.T. Owolabi, N.A.S. Aprilia, S. Rizal, H.P.S.A. Khalil, Development of seaweed-based bamboo microcrystalline cellulose films intended for sustainable food packaging applications, Bioresources 14 (2019) 3389–3410.
[6] N.A. Azlim, A. Mohammadi Nafchi, N. Oladzadabbasabadi, F. Ariffin, P. Ghalambor, S. Jafarzadeh, A.A. Al-Hassan, Fabrication and characterization of a pH-sensitive intelligent film incorporating dragon fruit skin extract, Food Sci. Nutr. 10 (2022) 597–608.
[7] S. Jafarzadeh, M. Zargar, M. Forough, Renewable and recyclable polymeric materials for food packaging: a new open special issue in materials, Materials 15 (2022) 5845.
[9] R. Syarifa, Y. Esmaeili, S. Jafarzadeh, F. Garavand, S. Mahmud, F. Ariffin, An investigation of the morphological, thermal, mechanical, and barrier properties of an active packaging containing micro-and nano-sized ZnO particles, Food Sci. Nutr. 11 (2023) 7373–7382.
[10] F. Garavand, S. Jafarzadeh, I. Cacciotti, N. Vahedikia, Z. Sarlak, Ö. Tarhan, S. Yousefi, M. Rouhi, R. Castro-Muñoz, S.M. Jafari, Different strategies to reinforce the milk protein-based packaging composites, Trends Food Sci. Technol. 123 (2022) 1–14.
[11] Z. Moslehi, A. Mohammadi Nafchi, M. Moslehi, S. Jafarzadeh, Aflatoxin, microbial contamination, sensory attributes, and morphological analysis of pistachio nut coated with methylcellulose, Food Sci. Nutr. 9 (2021) 2576–2584.
[12] S. Jafarzadeh, F. Ariffin, S. Mahmud, A.K. Alias, A. Najafi, M. Ahmad, CHARACTERIZATION OF SEMOLINA BIOPOLYMER FILMS ENRICHED WITH ZINC OXIDE NANO RODS, Ital. J. Food Sci. 29 (2017) 195–208.
[13] D.M. Nguyen, T.V.V. Do, A.-C. Grillet, H.H. Thuc, C.N.H. Thuc, Biodegradability of polymer film based on low density polyethylene and cassava starch, Int. Biodeterior. Biodegradation 115 (2016) 257–265.
[14] F. Garavand, I. Cacciotti, N. Vahedikia, A. Rehman, Ö. Tarhan, S. Akbari-Alavijeh, R. Shaddel, A. Rashidinejad, M. Nejatian, S. Jafarzadeh, A comprehensive review on the nanocomposites loaded with chitosan nanoparticles for food packaging, Crit. Rev. Food Sci. Nutr. 62 (2022) 1383–1416.
[15] S. Jafarzadeh, A.K. Alias, F. Ariffin, S. Mahmud, A. Najafi, S. Sheibani, Characterization of a new biodegradable edible film based on semolina loaded with nano kaolin, Int. Food Res. J. 24 (2017).
[16] S. Jafarzadeh, M. Forough, V.J. Kouzegaran, M. Zargar, F. Garavand, M. Azizi-Lalabadi, M. Abdollahi, S.M. Jafari, Improving the functionality of biodegradable food packaging materials via porous nanomaterials, Compr. Rev. Food Sci. Food Saf. 22 (2023) 2850–2886.
[17] J. Zhou, H. Liu, Y. Lin, C. Zhou, A. Huang, Synthesis of well-shaped and high-crystalline Ce-based metal organic framework for CO2/CH4 separation, Microporous Mesoporous Mater. 302 (2020) 110224.
[18] A. Lin, A.A. Ibrahim, P. Arab, H.M. El-Kaderi, M.S. El-Shall, Palladium nanoparticles supported on Ce-metal–organic framework for efficient CO oxidation and low-temperature CO2 capture, ACS Appl. Mater. Interfaces 9 (2017) 17961–17968.
[19] J. Zhao, F. Wei, W. Xu, X. Han, Enhanced antibacterial performance of gelatin/chitosan film containing capsaicin loaded MOFs for food packaging, Appl. Surf. Sci. 510 (2020) 145418.
[20] K. Chen, J. Yu, J. Huang, Q. Tang, H. Li, Z. Zou, Improved mechanical, water vapor barrier and UV-shielding properties of cellulose acetate films with flower-like metal-organic framework nanoparticles, Int. J. Biol. Macromol. 167 (2021) 1–9.
[21] M. Zhang, Y. Zheng, Y. Jin, D. Wang, G. Wang, X. Zhang, Y. Li, S. Lee, Ag@ MOF-loaded p-coumaric acid modified chitosan/chitosan nanoparticle and polyvinyl alcohol/starch bilayer films for food packing applications, Int. J. Biol. Macromol. 202 (2022) 80–90.
[22] Y.J. Bae, E.S. Cho, F. Qiu, D.T. Sun, T.E. Williams, J.J. Urban, W.L. Queen, Transparent metal–organic framework/polymer mixed matrix membranes as water vapor barriers, ACS Appl. Mater. Interfaces 8 (2016) 10098–10103.
[23] S. Feng, Q. Tang, Z. Xu, K. Huang, H. Li, Z. Zou, Development of novel Co-MOF loaded sodium alginate based packaging films with antimicrobial and ammonia-sensitive functions for shrimp freshness monitoring, Food Hydrocoll. 135 (2023) 108193.
[24] A. Mazloom-Jalali, Z. Shariatinia, I.A. Tamai, S.-R. Pakzad, J. Malakootikhah, Fabrication of chitosan–polyethylene glycol nanocomposite films containing ZIF-8 nanoparticles for application as wound dressing materials, Int. J. Biol. Macromol. 153 (2020) 421–432.
[25] C. Atzori, K.A. Lomachenko, S. Øien-Ødegaard, C. Lamberti, N. Stock, C. Barolo, F. Bonino, Disclosing the properties of a new Ce (III)-based MOF: Ce2 (NDC) 3 (DMF) 2, Cryst. Growth Des. 19 (2018) 787–796.
[26] S. Jafarzadeh, A.K. Alias, F. Ariffin, S. Mahmud, A. Najafi, M. Ahmad, Fabrication and characterization of novel semolina-based antimicrobial films derived from the combination of ZnO nanorods and nanokaolin, J. Food Sci. Technol. 54 (2017) 105–113.
[27] M. Jridi, S. Hajji, H. Ben Ayed, I. Lassoued, A. Mbarek, M. Kammoun, N. Souissi, M. Nasri, Physical, structural, antioxidant and antimicrobial properties of gelatin–chitosan composite edible films, Int. J. Biol. Macromol. 67 (2014) 373–379.
[28] N. Rabiee, M. Bagherzadeh, M. Kiani, A.M. Ghadiri, K. Zhang, Z. Jin, S. Ramakrishna, M. Shokouhimehr, High gravity-assisted green synthesis of ZnO

nanoparticles via Allium ursinum: conjoining nanochemistry to neuroscience, Nano Express 1 (2020) 020025.
[29] V.C. Anadebe, V.I. Chukwuike, S. Ramanathan, R.C. Barik, Cerium-based metal organic framework (Ce-MOF) as corrosion inhibitor for API 5L X65 steel in CO2-saturated brine solution: XPS, DFT/MD-simulation, and machine learning model prediction, Process. Saf. Environ. Prot. 168 (2022) 499–512.
[30] S. Jafarzadeh, A. Salehabadi, S.M. Jafari, 10 Metal Nanoparticles as Antimicrobial Agents in Food Packaging, 2020.
[31] M. Aslam, M.A. Kalyar, Z.A. Raza, Investigation of structural and thermal properties of distinct nanofillers-doped PVA composite films, Polym. Bull. 76 (2019) 73–86.
[32] S. Jafarzadeh, S.M. Jafari, Impact of metal nanoparticles on the mechanical, barrier, optical and thermal properties of biodegradable food packaging materials, Crit. Rev. Food Sci. Nutr. 61 (2021) 2640–2658.
[33] M.K.S. Monteiro, V.R.L. de Oliveira, F.K.G. dos Santos, E.L.B. Neto, R.H. de L. Leite, E.M.M. Aroucha, R.R. Silva, K.N. de O. Silva, Incorporation of bentonite clay in cassava starch films for the reduction of water vapor permeability, Food Res. Int. 105 (2018) 637–644.
[34] W. Zhang, M. Azizi-Lalabadi, S. Jafarzadeh, S.M. Jafari, Starch-gelatin blend films: a promising approach for high-performance degradable food packaging, Carbohydr. Polym. 121266 (2023).
[35] M. Azizi-Lalabadi, M. Alizadeh-Sani, B. Divband, A. Ehsani, D.J. McClements, Nanocomposite films consisting of functional nanoparticles (TiO2 and ZnO) embedded in 4A-Zeolite and mixed polymer matrices (gelatin and polyvinyl alcohol), Food Res. Int. 137 (2020) 109716.
[36] N. Vahedikia, F. Garavand, B. Tajeddin, I. Cacciotti, S.M. Jafari, T. Omidi, Z. Zahedi, Biodegradable zein film composites reinforced with chitosan nanoparticles and cinnamon essential oil: physical, mechanical, structural and antimicrobial attributes, Colloids Surf. B: Biointerfaces 177 (2019) 25–32.
[37] E.W.N. Chong, S. Jafarzadeh, M.T. Paridah, D.A. Gopakumar, H.A. Tajarudin, S. Thomas, H.P.S. Abdul Khalil, Enhancement in the physico-mechanical functions of seaweed biopolymer film via embedding fillers for plasticulture application—a comparison with conventional biodegradable mulch film, Polymers (Basel) 11 (2019) 210.
[38] T. Mohammadi-Moghaddam, M. Kariminejad, S. Hadad, S. Jafarzadeh, D. Shahrampour, Physical properties, antioxidant activity, and antimicrobial properties of edible film prepared from black plum peel extract as a valuable by-product of plum processing, J Food Chem Nanotechnol 9 (2023) 156–162.
[39] K. Jantanasakulwong, N. Homsaard, P. Phengchan, P. Rachtanapun, N. Leksawasdi, Y. Phimolsiripol, C. Techapun, P. Jantrawut, Effect of dip coating polymer solutions on properties of thermoplastic cassava starch, Polymers (Basel) 11 (2019) 1746.
[40] S. Kiatkamjornwong, P. Thakeow, M. Sonsuk, Chemical modification of cassava starch for degradable polyethylene sheets, Polym. Degrad. Stab. 73 (2001) 363–375.
[41] S.H. Clasen, C.M.O. Müller, A.L. Parize, A.T.N. Pires, Synthesis and characterization of cassava starch with maleic acid derivatives by etherification reaction, Carbohydr. Polym. 180 (2018) 348–353.
[42] C. Healy, K.M. Patil, B.H. Wilson, L. Hermanspahn, N.C. Harvey-Reid, B.I. Howard, C. Kleinjan, J. Kolien, F. Payet, S.G. Telfer, The thermal stability of metal-organic frameworks, Coord. Chem. Rev. 419 (2020) 213388.
[43] P. Kampeerapappun, D. Aht-Ong, D. Pentrakoon, K. Srikulkit, Preparation of cassava starch/montmorillonite composite film, Carbohydr. Polym. 67 (2007) 155–163.
[44] N.A. Khan, M.B.K. Niazi, F. Sher, Z. Jahan, T. Noor, O. Azhar, T. Rashid, N. Iqbal, Metal organic frameworks derived sustainable polyvinyl alcohol/starch nanocomposite films as robust materials for packaging applications, Polymers (Basel) 13 (2021) 2307.
[45] S. Jafarzadeh, A.K. Alias, F. Ariffin, S. Mahmud, Physico-mechanical and microstructural properties of semolina flour films as influenced by different sorbitol/glycerol concentrations, Int. J. Food Prop. 21 (2018) 983–995.
[46] M. Safarkhani, B. Farasati Far, E.C. Lima, S. Jafarzadeh, P. Makvandi, R.S. Varma, Y. Huh, M. Ebrahimi Warkiani, N. Rabiee, Integration of MXene and microfluidics: a perspective, ACS Biomater Sci Eng 10 (2024) 657–676.
[47] Y. Xiao, Z. Li, A. Bianco, B. Ma, Recent advances in calcium-based anticancer nanomaterials exploiting calcium overload to trigger cell apoptosis, Adv. Funct. Mater. 33 (2023) 2209291.
[48] I. Shahabi-Ghahfarrokhi, F. Khodaiyan, M. Mousavi, H. Yousefi, Green bionanocomposite based on kefiran and cellulose nanocrystals produced from beer industrial residues, Int. J. Biol. Macromol. 77 (2015) 85–91.